Shear Banding in Biphasic Liquid-Liquid Systems

Sergio Caserta, Marino Simeone, and Stefano Guido*

Dipartimento di Ingegneria chimica, Università di Napoli Federico II, Napoli 80125, Italy

(Received 8 November 2007; published 3 April 2008)

In this Letter, we present the first systematic report of shear-induced banding in microconfined biphasic liquid-liquid systems, i.e., formation of alternating regions of high and low volume fraction of dispersed-phase droplets in a parallel plate flow cell. Such a flow-driven, gap-dependent phenomenon is only observed at low values of the viscosity ratio between the dispersed and the continuous phase, and in a given range of the applied shear rate. Based on rheological measurements, band formation is found to be associated with a viscosity decrease as compared to the homogeneous, structureless case, thus showing that system microstructure is somehow evolving towards reduced viscous dissipation under shear flow.

DOI: 10.1103/PhysRevLett.100.137801 PACS numbers: 61.25.−f, 68.05.Cf, 83.50.−v, 83.85.Ei

Flow-induced pattern formation leading to banded regions is a quite general phenomenon in complex fluids, being found in wormlike micellar solutions [1], rodlike virus suspensions [2], attractive emulsions [3], lyotropic liquid crystals [4], suspensions of rigid spherical particles [5], supramolecular polymer solutions [6], and granular materials [7]. Band formation in complex fluids has been mostly studied in shear flow, which is shown schematically in Fig. 1 in the simplest situation of two parallel plates, the lower being translated with velocity V with respect to the upper, with the sample placed in between. In this flow geometry, the imposed rate of deformation or shear rate $\dot{\gamma}$ is given by the ratio between V and the gap size δ between the plates. Depending on the material under investigation, formation of bands alternating along either of the three axes of shear flow depicted in Fig. 1, i.e., flow direction x, velocity gradient y, and vorticity axis z, has been reported. Although this diverse phenomenology is still puzzling, so far possible mechanisms of band formation have been associated with complex physicochemical interactions, such as in attractive emulsions, where droplets flocculate due to micellar depletion attractions, and with non-Newtonian properties of the continuous phase, such as in particle suspensions in viscoelastic media. Furthermore, a possible role of curvature in the shear flow field (such as in the concentric cylinder geometry, where spatial gradients of $\dot{\gamma}$ are present) has also been advocated.

As compared to previous studies, we show here that band formation is found in the relatively simpler situation of a mixture of two Newtonian, immiscible liquid phases with no interfacial agents, and undergoing shear flow between two sliding parallel plates, such as in Fig. 1, where curvature effects are ruled out. This finding points to some basic, gap-dependent fluidodynamic interactions as underlying the banding phenomenon. In biphasic liquid systems, an applied external flow affects system microstructure, i.e., size and shape distribution of the dispersed-phase droplets, by two main mechanisms: droplet deformation [8], which can eventually lead to breakup in smaller fragments [9], and collision [10], which may elicit coalescence into larger droplets [11]. In turn, flow-induced microstructure evolution may affect the flow field itself, thus modifying rheological properties, such as sample viscosity. Recently, wall effects on droplet deformation, breakup and coalescence, being relevant for microfluidics applications, have been addressed in several studies [12,13]. In particular, an intriguing droplet-string transition and stable pearl-necklace structures have been observed in equiviscous polymer blends sheared in a parallel plate apparatus when the average droplet radius is comparable to gap size [12]. However, observations of shear banding in biphasic liquid systems are lacking.

In this work, immiscible polymer blends of silicone oil in polybutene (continuous phase, viscosity $\eta_c = 88$ Pa s), with volume fractions Φ ranging from 2.5% to 20% and viscosity ratios λ from 0.002 to 1, are used as a model system (the viscosity ratio is tuned by mixing silicone oils of different viscosity). The samples are sheared in a flow apparatus consisting of two parallel plates made of optical glass and an optical microscope equipped with a CCD video camera (a detailed description is found elsewhere [10]). Rheological tests are carried out both in a constant-stress and in a strain-controlled rheometer with cone-and-plate geometry. Both the polymers used in the experiments exhibit Newtonian behavior in the shear rate range investigated (between 0.05 and 1 s^{-1}). The interfacial tension σ is equal to 2 mN/m [9].

At viscosity ratios of 1 and above, the sample looks homogeneous throughout the whole shear experiment (up to 100 000 strain units). The appearance of bands with droplet-rich and depleted regions alternating along the vorticity axis [i.e., the z axis in Fig. 1(a)] is only noticed when blends of low viscosity ratio λ (below 1) are extensively sheared within a given range of shear rate. An example is shown in Figs. 1(b)–1(e), where a sequence of low magnification micrographs taken during flow at increasing values of strain is presented for a 10% v/v blend with a viscosity ratio of 0.04. Starting from a spatially uniform distribution of droplets [Fig. 1(b)], band formation

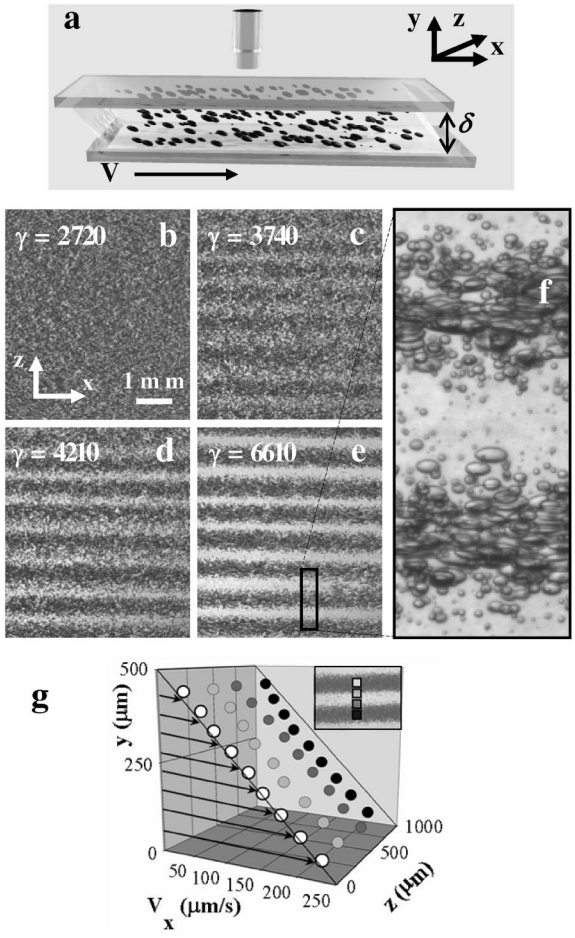

FIG. 1. Images of a 10% v/v sample sheared at $\dot{\gamma} = 0.5\ s^{-1}$ and observed along the velocity gradient direction (y-axis). The strain $\gamma = \dot{\gamma}t$, which is a measure of displacement relative to the gap between the plates, increases from (b) to (e). Band structure is shown in more detail in (f) by enlarging the rectangular frame in (e). The 3D plot in (g) shows velocity profiles across droplet-rich and depleted areas within the bands, which are marked in the inset as gray squares. $\lambda = 0.04$, $\delta = 500\ \mu$m.

becomes more and more apparent as the sample is sheared [Figs. 1(c)–1(e)], until an almost complete separation between droplet-rich and droplet-devoid regions is reached, as shown in the enlarged view in Fig. 1(f).

To evaluate if band formation is associated with regions of high and low shear rate, such as in velocity gradient banding [1], velocity profiles are measured during flow both before and after the appearance of the banded structure. Some results in the latter case are presented in Fig. 1(g), where a 3D plot is used to represent velocity vs y axis at four different sample locations along the vorticity axis z. The four locations, which span an entire band period, are shown as gray squares in the inset of Fig. 1(g). The four velocity profiles are linear and all lie on the same plane going from the top to the bottom plate of the shearing device, thus showing that the shear flow field is indeed homogeneous throughout the sample.

To elucidate the 3D structure of the shear bands, high magnification optical sectioning and sample scanning is performed by stopping the flow after band formation. An example of 3D image reconstruction from multiple stacks of images, which have been processed to extract droplet size and location within the sampled volume [14], is presented in Fig. 2(a). From the reconstructed view, droplet size and volume fraction appears to be maximal in the dispersed phase-rich regions and to decrease to a minimum in the continuous phase-rich ones. This is confirmed by the quantitative measurement of the number average droplet diameter $D_{1,0}$ as a function of the vorticity axis z [see Fig. 2(b)], which exhibits an alternating trend in parallel to the band structure. In the same plot, the average capillary number $\mathrm{Ca} = D_{1,0}\eta_c\dot{\gamma}/2\sigma$, which is shown in the right-hand axis, is well below the critical value for droplet breakup under shear flow (0.54 at $\lambda = 0.1$ [9]). Thus, the main mechanisms acting to modify system microstructure in our experiments are flow-induced droplet deformation, collision, and coalescence, the latter being favored at low Ca. The higher average droplet size in the droplet-rich bands can be attributed to the enhanced coalescence rate at increasing droplet volume fractions, an effect which is due to higher collision frequency and is well documented in the literature [11]. A mechanism of size segregation due to droplet collisions, in analogy with the ordered spatial distribution observed in sheared polydisperse granular systems [7], can also be at play due to hydrodynamic interactions [15].

A visual representation of band evolution can be obtained by calculating the x-averaged image gray level as a

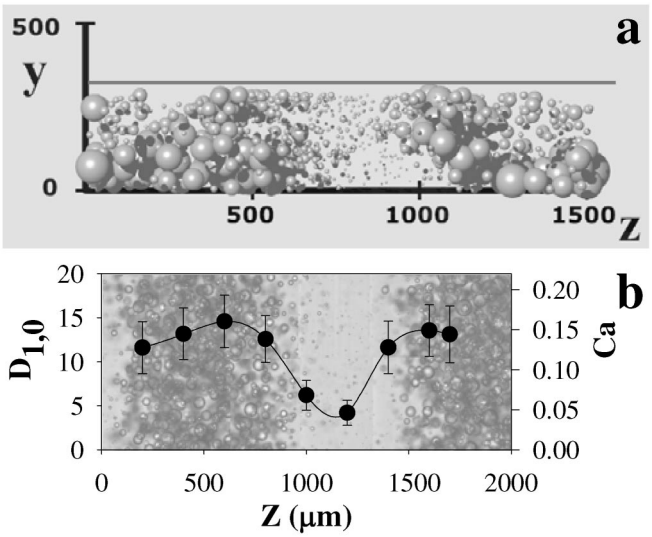

FIG. 2. A 3D reconstruction based on stacks of images acquired along the y axis upon stopping the flow after band formation. The picture shows the y-z projection of the sampled volume. The number average $D_{1,0}$ and Ca, based on the quantitative analysis of 30 z stacks, are plotted in (b) as a function of z and superimposed to a composite image of the scanned area. $\lambda = 0.1$, $\dot{\gamma} = 0.5\ s^{-1}$, $\Phi = 10\%$ v/v.

function of strain. This is shown in Figs. 3(a) and 3(b), where the x-averaged gray level is plotted as a function of z and strain at a gap size of 250 and 500 μm, respectively. In the initial stage of the experiment the sample is homogeneous and, apart from some fluctuations, no structure in the gray level spatial distribution is observed. At some point, a pattern of alternating darker and lighter regions becomes visible, which can be taken somehow as the onset of band formation, and is well represented by a simple sinusoidal fit. This pattern can also be taken as a qualitative representation of the droplet volume fraction distribution within the sample at each strain. Fourier-transform based image analysis shows that band kinetics and spacing are strong increasing functions of gap size, the latter more than doubling in going from 250 to 500 μm gap size (data not shown for the sake of brevity).

The effect of lowering the viscosity ratio is illustrated in Fig. 4, where a composite image (i.e., obtained by combining adjacent images acquired through sample scanning in the x-y plane) is shown at $\lambda = 0.01$. At such value of the viscosity ratio, parallel pearl-necklace structures extending along the vorticity direction are superimposed to the bands aligned in the flow direction and described so far. The enlargement presented in the inset of Fig. 4 shows in more detail the droplets constituting the pearl necklaces and the bands. By looking at the evolution of the sample under shear flow, both structures appear to form at about the same strain value. At even lower values of λ, no bands are observed and large droplets oriented along flow direction are generated as a result of coalescence. Such droplets are quite elongated and are stabilized against breakup by the confining walls [12,13].

In addition to optical experiments, rheological tests are also performed by using a cone-and-plate rotational geometry, which is schematically represented in the inset of Fig. 5(a). Data of blend viscosity η (normalized with respect to the initial value η_0) vs strain under extensive shearing (over 20 000 strain units) are plotted in Fig. 5(a) at different viscosity ratios. While viscosity stays constant with strain at a viscosity ratio of 1, a significant decrease is observed both at $\lambda = 0.1$ and 0.04, the latter displaying a faster kinetics, until a plateau value is eventually reached. The data in Fig. 5(a) refer to measurements done in a constant-stress rheometer, but no significant change is observed by using a strain-controlled instrument. By carefully lifting the cone, a concentric banded structure alternating along the vorticity direction is observed, as shown in Fig. 5(b), which corresponds to a viscosity ratio of 0.1 (on the contrary, the sample at $\lambda = 1$ looks structureless). The spacing between the concentric bands increases from the center to the edge of the plate, as it does the gap between the cone and the plate. This finding is in agreement with the increase of band spacing with gap size already described for the sliding plate device. In Figs. 5(c)–5(e) images of a 10% v/v sample at $\lambda = 0.1$ sheared in the sliding plate device are shown at increasing values of strain for comparison with the viscosity plot of Fig. 5(a). The higher sample transparency due to the small value of the gap size (250 μm) allows detailed microscopic observations down to individual droplet level. Upon inception of flow, the initial structureless morphology [Fig. 5(c)] evolves by formation of droplet clusters [Fig. 5(d)], which grow up to the size of the gap and connect together along the flow direction, thus creating the gap-dependent banded structure [Fig. 5(e)]. Droplet clustering corresponds to the decreasing part of the viscosity vs strain plot in Fig. 5(a), while the well-formed banded structure is observed within the viscosity plateau. In fact, the shear banded structure appears quite stable, being still observed after extensive shearing (up to 230 000 strain units at $\lambda = 0.1$). Furthermore, droplet size within the bands appears to level off after band formation.

The droplet-rich and depleted regions observed in the banded structure correspond to high and low viscosity values, respectively, (being viscosity an increasing function of Φ in the range investigated). Since shear rate was found to be homogeneous within the sample (at variance with gradient banding), this work provides a direct evidence of the coexistence of regions with different values of shear stress ($= \eta\dot{\gamma}$) in vorticity banding. Such coexistence has been hypothesized in the case of vorticity banding in lyotropic liquid crystals [4], but not confirmed by direct optical microscopy observations so far.

The images of Fig. 5 provide some insight on the mechanisms governing band formation at low viscosity ratios by showing droplet clustering as an intermediate

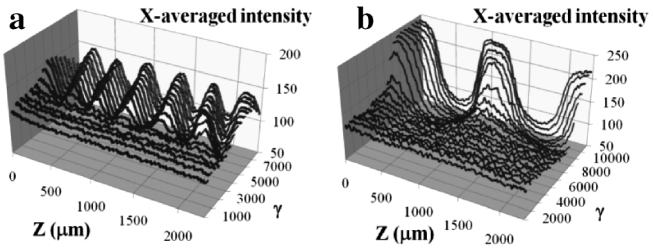

FIG. 3. 3D plots of x-averaged gray level vs z and strain at gap size = 250 and 500 μm, respectively. $\lambda = 0.1$, $\dot{\gamma} = 0.5\ s^{-1}$, $\Phi = 10\%$ v/v.

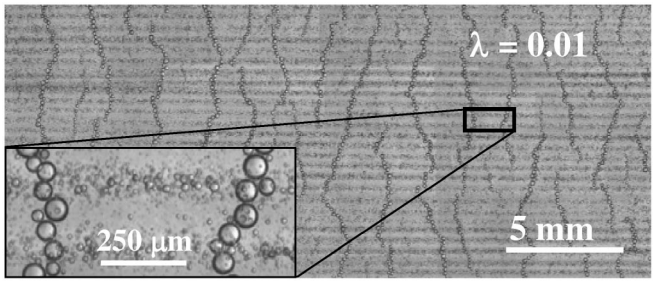

FIG. 4. A composite image at $\lambda = 0.01$ showing pearl-necklace structures perpendicular to flow direction together with the vorticity shear bands. An enlarged view of the square frame is shown in the inset.

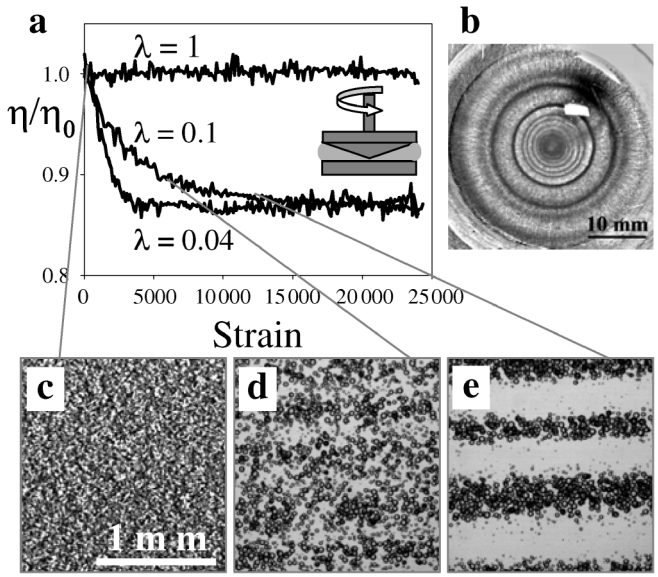

FIG. 5. (a) Viscosity vs strain under extensive shearing at $\lambda = 1$, 0.1, and 0.04 as measured in the cone-and-plate geometry (shown in the inset). (b) a picture of the sample taken after gently raising the cone. (c)–(e) consecutive images of band formation in the sliding plate device at $\lambda = 0.1$ and $\dot{\gamma} = 0.5\ s^{-1}$. $\Phi = 10\%$ v/v and gap $\delta = 250\ \mu m$.

stage of the shear banding phenomenon. Once formed as a result of droplet collisions, the clusters are stabilized by the associated reduction of viscous dissipation with respect to the homogeneous case. This proposed scenario of band formation is in line with recent perspectives on the mechanisms governing noise to order transitions [16], which share as common elements a randomizing effect (here diffusion due to droplet collisions) and a source of dissipation (here associated to viscous effects). The absence of banding at high viscosity ratios can be related to the lack of the viscosity-induced stabilizing effect [see Fig. 5(a)]. Hydrodynamic interactions may also play a role by lowering collision efficiency with increasing λ [15]. The lack of band formation at the lowest viscosity ratio investigated (i.e., $\lambda = 0.002$) can be attributed to the competing effect of coalescence which is higher the lower is the value of λ [17], and can then elicit the formation of large, wall-stabilized droplets [12]. The formation of the pearl necklaces structures coexisting with shear bands at $\lambda = 0.01$ remains, however, unexplained. Within this framework, the fact that band formation is only found in a given range of shear rate can be explained by the opposing actions of (1) shear-induced droplet diffusion tending to randomize the droplet spatial distribution at high values of $\dot{\gamma}$ [18] and (2) droplet coalescence, whose rate increases upon lowering $\dot{\gamma}$ [17]. As compared to the string and pearl necklaces morphologies [12], which have been reported at a viscosity ratio of 1, shear bands are observed at smaller values of λ and of the ratio between droplet radius and gap size [see Fig. 2].

In conclusion, shear banding in biphasic liquid systems appears as an intriguing novel phenomenology, being relevant to the study of the interplay between flow and microstructure, which is an important issue in the processing of these systems. In particular, possible applications of banded textures in biphasic liquid systems can be envisaged in microfluidics devices, where droplets can be used as microreactors or as carriers of a component insoluble in the continuous phase [19], and the development of techniques to manipulate droplet spatial distribution is at order.

Financial support from the Italian Ministry of Research under the PRIN 2006 program is gratefully acknowledged. The authors wish to thank A. Ferrara and A. D'Amato for their help in the experimental part, and Professor G. Marrucci for useful discussions.

*stefano.guido@unina.it

[1] N. A. Spenley, M. E. Cates, and T. C. B. McLeish, Phys. Rev. Lett. **71**, 939 (1993).
[2] K. Kang, M. P. Lettinga, Z. Dogic, and J. K. G. Dhont, Phys. Rev. E **74**, 026307 (2006).
[3] M. Simeone, V. Sibillo, M. Tassieri, and S. Guido, J. Rheol. (N.Y.) **46**, 1263 (2002); A. Montesi, A. A. Pena, and M. Pasquali, Phys. Rev. Lett. **92**, 058303 (2004).
[4] G. M. H. Wilkins and P. D. Olmsted Eur. Phys. J. E **21**, 133 (2006).
[5] D. Highgate, Nature (London) **211**, 1390 (1966).
[6] J. van der Gucht, M. Lemmers, W. Knoben, N. A. M. Besseling, and M. P. Lettinga, Phys. Rev. Lett. **97**, 108301 (2006).
[7] M. P. Ciamarra, A. Coniglio, and M. Nicodemi, Phys. Rev. Lett. **94**, 188001 (2005).
[8] G. I. Taylor, Proc. R. Soc. A **138**, 41 (1932).
[9] V. Cristini, S. Guido, A. Alfani, J. Blawzdziewicz, and M. Loewenberg, J. Rheol. (N.Y.) **47**, 1283 (2003).
[10] S. Guido and M. Simeone, J. Fluid Mech. **357**, 1 (1998).
[11] U. Sundararaj and C. W. Macosko, Macromolecules **28**, 2647 (1995).
[12] K. B. Migler, Phys. Rev. Lett. **86**, 1023 (2001); J. A. Pathak, C. M. Davis, S. D. Hudson, and K. B. Migler, J. Colloid Interface Sci. **255**, 391 (2002).
[13] V. Sibillo, G. Pasquariello, M. Simeone, V. Cristini, and S. Guido, Phys. Rev. Lett. **97**, 054502 (2006); A. Vananroye, P. V. Puyvelde, and P. Moldenaers, Langmuir **22**, 2273 (2006).
[14] S. Caserta, M. Simeone, and S. Guido, Rheol. Acta **43**, 491 (2004).
[15] H. Wang, A. Z. Zinchenko, and R. H. Davis, J. Fluid Mech. **265**, 161 (1994).
[16] T. Shinbrot and F. J. Muzzio, Nature (London) **410**, 251 (2001).
[17] S. P. Lyu, F. S. Bates, and C. W. Macosko, AIChE J. **48**, 7 (2002).
[18] M. Loewenberg and E. J. Hinch, J. Fluid Mech. **338**, 299 (1997).
[19] M. Joanicot and A. Ajdari, Science **309**, 887 (2005); S. Haeberlea and R. Zengerle, Lab Chip **7**, 1094 (2007).